Hybrid electroluminescent devices composed of (In,Ga)N micro-LEDs and monolayers of transition metal dichalcogenides

K. Oreszczuk[1], J. Slawinska[2], A. Rodek[1], M. Potemski[1,3], C. Skierbiszewski[2], and P. Kossacki[1]

[1] *Institute of Experimental Physics, Faculty of Physics,*
University of Warsaw, Pasteura 5, 02-093 Warsaw, Poland
[2] *Institute of High Pressure Physics, Polish Academy of Sciences, Sokołowska 29/37, 01-142 Warsaw, Poland and*
[3] *Laboratoire National des Champs Magnétiques Intenses,*
CNRS-UGA-UPS-INSA-EMFL, 25 rue des Martyrs, 38042 Grenoble, France

We demonstrate a novel electro-luminescence device in which GaN-based μ-LEDs are used to trigger the emission spectra of monolayers of transition metal dichalcogenides, which are deposited directly on μ-LED surface. A special μ-LED design enables the operation of our structures even in the limit of low temperatures. A device equipped with a selected WSe$_2$ monolayer flake is shown to act as a stand-alone, electrically-driven single-photon source.

PACS numbers:

I. INTRODUCTION

Atomically thin semiconductors, such as monolayers of transition metal dichalcogenides (TMDs) and their homo- and hetero-structures, exhibit interesting optical properties. The list of prominent attributes of these two-dimensional (2D) structures includes: strong excitonic binding[1–3] which favors room temperature capabilities[4], possibilities to manipulate the valley degree freedom[5–8], and emergence of new class of quantum emitters[9–15]. In parallel to the intense fundamental research, pertinent efforts are also undertaken to exploit the TMD semiconductors in designing and fabricating of new optoelectronic devices of possible practical use[16,17]. The operation of such devices is desired to be electrically driven. Controlled doping of TMD materials, although essential for the operation of conventional electroluminescent p-n diodes, still remains a largely unresolved challenge[18–20].

Therefore, alternative methods are being developed, relying most often on tunneling mechanisms of carrier injection into the active 2D component of the device. In fact, the electrically driven emission from TMD semiconductors has been successfully demonstrated in a number of differently designed structures[21–27]. However, the architecture of such structures implies rather complex manufacturing processes, and the performance of the reported devices remains not yet fully satisfying. This calls for further efforts to improve/optimize the already proposed device schemes and/or to search for optional solutions.

Taking advantage of the advanced technology of nitrides[28], we put here forward a new concept of a compact pseudo-electroluminescent device by integrating the TMD semiconductors into (In,Ga)N light-emitting diodes (LEDs). Our devices are composed of micro-(In,Ga)N-LEDs (μ-LEDs), on top of which we directly deposit the TMD layers: the electrically driven (In,Ga)N μ-LEDs serve as the excitation sources to generate the PL emission from TMDs. A special design of our (In,Ga)N diodes ensures their functionality at cryogenic temper-

atures, which are preferential conditions for generating light from TMD monolayers and an unavoidable requirement when tracing the quantum emission centres from these layers. Low-temperature operation of our electroluminescent devices comprised of different: MoS$_2$, MoSe$_2$, WSe$_2$ and WS$_2$ monolayers, is demonstrated. Importantly, the hybrid (In,Ga)N-μ-LED/WSe$_2$-monolayer device is also shown to function as an electrically driven source of single photons. While the fabrication of the present devices implies a laborious exfoliation manufacturing, we speculate that the industrial scalability of such devices could be approached in the future, taking into account the progress in the growth of TMDs by epitaxy methods and thus evoking a possibility to grow the TMDs directly on (In,Ga)N LEDs, particularly with molecular beam epitaxy techniques[29].

The technology of nitride LEDs has undergone intense development in recent years[28]. Relevant efforts have been made to respond to pertinent demands for low energy consumption, that is, to achieve high luminous efficacy of LEDs, but also to improve their brightness and contrast, their shock resistance, and degradation time[28]. Although many nitride LEDs already find relevant applications in display technology[30,31], the new possibilities for nitride optoelectronics have been raised more recently by employing a scheme of a tunnel junction (TJ)[32–34]. Such architecture of (In,Ga)N LEDs is also crucial for the present work. The buried TJ enables the nitride LEDs to operate at cryogenic temperatures[35]. Equally important is that the use of the TJ allows us to replace the top p-type layer (of a conventional LED) with a highly conductive n-type layer. This enhances the current spreading and enables the n-type application of the side contacts to the device. Thus, TMD flakes can be directly deposited on the GaN surface, and the experiments can be carried out at low temperatures.
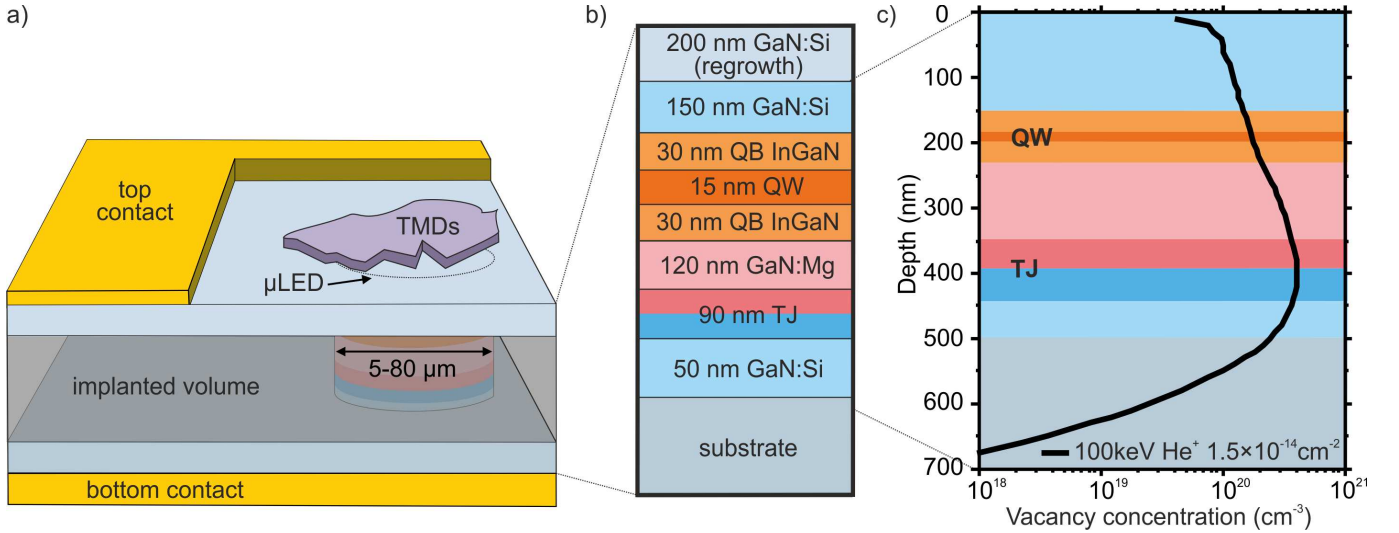
FIG. 1: (a) Schematic of the hybrid (In,Ga)N μ-LED/TMD-monolayer device. (b) Sketch of the nitride μ-LED structure grown by plasma assisted molecular beam epitaxy, with a characteristic sequence of epitaxial sections. (c) Ion-implantation profile for the implemented He$^+$ energy of 100 keV and dose of $1.5 \cdot 10^{14}$ cm^{-2}.

II. EXPERIMENTAL DETAILS

The epitaxial structure, schematically shown in Figure 1, was grown by plasma-assisted molecular beam epitaxy (PAMBE) on (0001) bulk GaN crystals. The PAMBE grown TJ (90 nm) and μ-LED structure that emits light at a wavelength of 450 nm was capped with the n-type GaN of 150 nm (Figure 1b). The emission area of μ-LEDs was defined by a photolithography mask and He$^+$ implantation (100 keV, $D = 1.5 \cdot 10^{14}$ cm^{-2}) of the μ-LED structure. Ion energy and dose were adjusted to penetrate the region at the location of the TJ (Figure 1c). The vacancies produced during the ion implantation of the TJ deteriorate the p-type and n-type conductivity and significantly increase the resistance of the TJ in the areas outside the μ-LEDs. After the ion implantation, the regrowth of 200 nm of high conductive n-type GaN enhances the current spreading at the top of μ-LEDs and allows the creation of the side contacts to the device. After regrowth, the 150×300 μm devices containing arrays of individual microdevices were separated by reactive-ion etching. Next, on the Ga-polar side of the samples, the Ti/Al/Ni/Au metal contact was deposited with a photolithographic mask, followed by lift-off. The same metal contacts were used for bottom contact on the nitrogen polar side.

The TMD monolayers have been placed on top of (In,Ga)N μ-LEDs (see Figure 1a) using deterministic transfer procedures. Monolayer flakes were mechanically exfoliated from bulk crystals with chemically pure back-grinding tape and transferred to the μ-LED surface using Gel-Pak DGL-X4 elastomeric films. A number of devices have been fabricated, comprising different, MoS$_2$, MoSe$_2$, WSe$_2$ and WS$_2$ monolayers.

The optical measurements were carried out in the two experimental configurations. Time-integrated studies were performed with the samples placed in the cold-finger cryostat. The emission of TMD monolayers has been measured in two different configurations. Primarily, the measurements have been carried out using the external laser excitation at 532 nm (2330 meV). Secondly, the luminescence was triggered from underneath with (In,Ga)N μ-LEDs.

The spectra composed of sharp emission lines characteristic of a WSe2 monolayer have also been examined with photon correlation experiments. These experiments have been carried out in the Hanbury-Brown-Twiss configuration, under (In,Ga)N LED excitation, and required the device to be immersed in superfluid helium to minimize the undesirable effects of heating (when large currents are driven to trigger the (In,Ga)N LEDs).

III. RESULTS AND DISCUSSION

The optical microscopy images of four different, WSe$_2$, MoSe$_2$, WS$_2$ and MoS$_2$ monolayers deposited on top of individual (In,Ga)N μ-LEDs are illustrated in Figure 2a-d. The characteristic, low temperature (10 K) microluminescence spectra of these layers are shown, correspondingly, in Figure 2e-h. The spectra shown with blue traces were measured under excitation with the external laser (532 nm), whereas those shown in red have been activated by the underneath (In,Ga)N μ–LEDs. The photoluminescence signals measured under external excitation are typical (with respect to spectral shape and characteristic energies and intensities) of TMD monolayers, as often studied when they are directly deposited on conventional
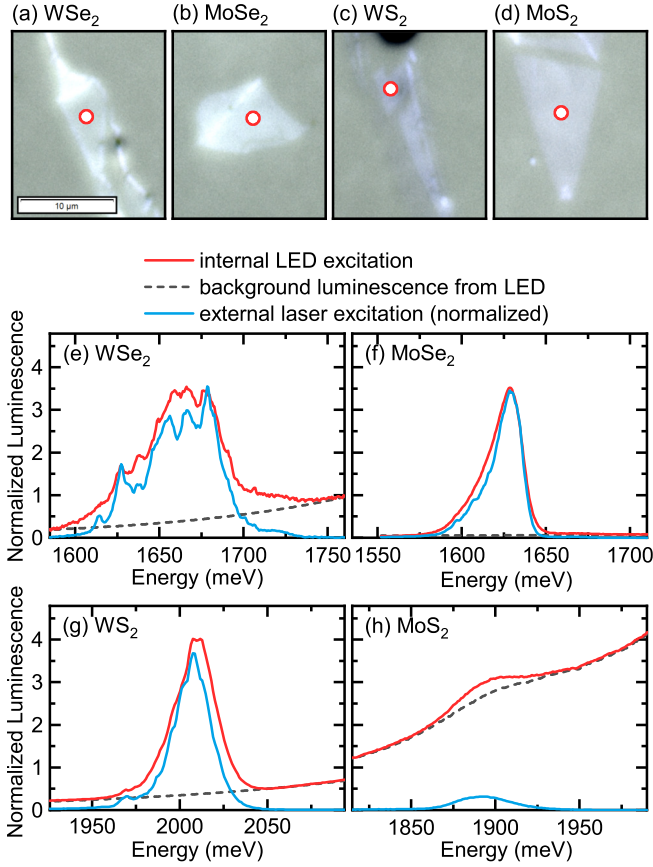
FIG. 2: (a-d) Images of the four different monolayers of TMDs. The flakes are exfoliated on µ-LEDs, which span the whole photo area. The µ-LED current density is equal to $0.3\,\mu\mathrm{A}\,\mu\mathrm{m}^{-2}$. Red circles mark the area from which the luminescence was acquired. (e-h) Spectra of the monolayers acquired under µ-LED excitation (red) and 532 nm (2330 meV) external laser excitation (blue). Dashed line: µ-LED luminescence acquired at the off-flake spot on the sample.
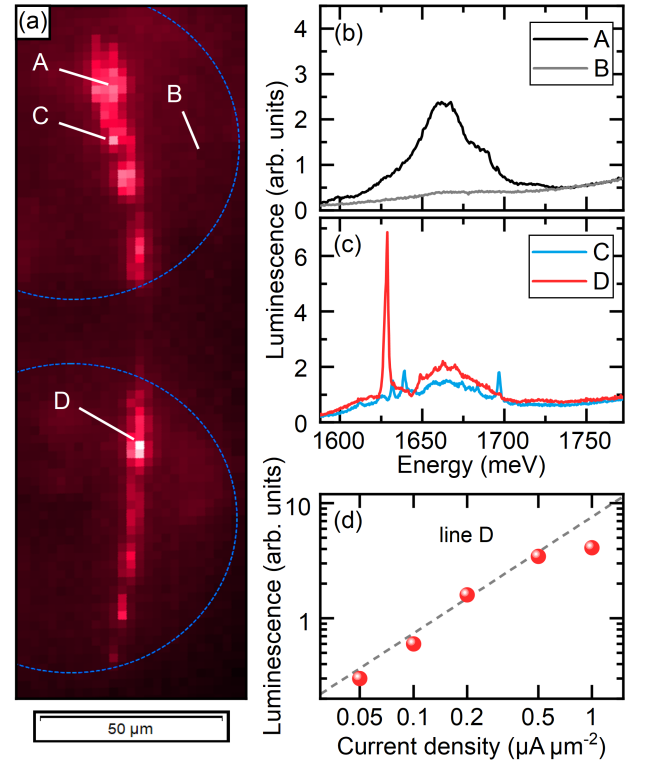
FIG. 3: (a) Map of the luminescence of a long and narrow flake of a monolayer WSe$_2$. The signal is integrated over 1625 meV - 1640 meV range, at the µ-LED current density of $0.5\,\mu\mathrm{A}\,\mu\mathrm{m}^{-2}$. Blue circles mark the outlines of the two circular µ-LEDs. Symbols A-D mark the spots presented in panels (b-c). (b) µ-LED excited PL of the homogeneous part of the WSe$_2$ flake (black) and the background luminescence of the µ-LED (grey). (c) µ-LED excited PL from the two spots with the narrow-line emitters. (d) The dependence of the luminescence intensity of line D on the µ-LED current density. The excitation sublinearity is caused by the elevated sample surface temperature at the highest current densities.

Si/SiO$_2$ substrates. Characteristic spectra of our WSe$_2$, MoSe$_2$ and WS$_2$ monolayers are fairly well reproduced when they are excited with (In,Ga)N µ-LEDs. On the other hand, the apparent background signal (see dashed traces in Figure 2e-f), which is due to an unfiltered low-energy tail of the (In,Ga)N emission, largely distorts the spectrum of the MoS$_2$ monolayer. This is, in fact, because of a rather weak luminescence efficiency of MoS$_2$ monolayers, as commonly reported when this particular TMD monolayer is not protected by hexagonal boron nitride.

Having established the overall functionality of our pseudo-electroluminescence devices, we now turn our attention to structures displaying sharp emission lines, possibly comprising the quantum emitter centers. Such centers preferentially appear in WSe$_2$ layers. Several µ-(In,Ga)N-LED/WSe$_2$-monolayer devices have been fabricated and tested. The irregular shape of WSe$_2$ flakes has been found to favour the observation of sharp emis-

sion lines. One may speculate this is due to the increased probability of the formation of the specific centers trapping the photoexcited carries at the edges of TMD flakes[9,10] or induced by inhomogenous strain distribution[11–15].

The representative example of a device displaying sharp emission lines contains a narrow, elongated flake of a WSe$_2$ monolayer. The device has been mounted on a cold finger of the cryostat, cooled down to 10 K and primarily tested under such conditions. After turning on the (In,Ga)N diodes, the emission spectra, in the spectral range 1590 − 1775 meV, were measured when scanning the surface of the WSe$_2$ flake and its surrounding, with a spatial resolution of 2 µm. A map of the intensity of the PL integrated over the spectral range of 1625 − 1640 meV is shown in Figure 3a. This image illustrates well the shape of the flake, which extends over the active areas of two neighbouring (In,Ga)N µ-LEDs. The background

signal due to the emission tail of the (In,Ga)N diode is
fairly weak - see the spectrum measured outside the flake
area (Figure 3b). The spectra measured in the areas in
the middle of the flake, away from its edges, exhibit a
broad feature, centered at 1660 meV – a typical response
of WSe$_2$ ML with significant spatial inhomogeneity (see
Figure 3b). However, near the edges and narrow parts
of the flake, the luminescence spectra often display sharp
lines; see Figure 3c.

Notably, the low activation current (below 1 nA μm^{-2})
of our device permits the measurements of the emission
spectra of the WSe$_2$ monolayer over a broad range of cur-
rent densities driving the (In,Ga)N diodes and thus en-
ables the straightforward tuning of the excitation power
to match the saturation point of a particular emitter. To
illustrate this effect, we present a typical PL intensity
of the emitter as a function of the current density (Fig-
ure 3d). As the luminescence intensity of narrow lines in
WSe$_2$ monolayers is known to drop down upon increase
of temperature[36] we conclude that the observed effect is
likely due to a low cooling efficiency of our device under
the current arrangement (limited by the heat transfer ef-
fectiveness between our device and the mounting base in
the cryostat). However, the heat generation process can
be suppressed by reducing the size of the μ-LED and the
precise positioning of the TMD flakes.

To demonstrate the operation of our device as a single-
photon source, the device was immersed in a superfluid
helium bath and cooled down to a temperature of 1.65 K.
This resulted in an improved cooling efficiency of the de-
vice, enabling the application of higher diode currents,
and at the same time gaining higher emission intensities
of narrow emission lines. This allowed for the correlation
measurements of the photon statistics emitted from the
particular centre.

In Figure 4a we present the spectrum of the narrow
line emitter in the WSe$_2$ monolayer under the (In,Ga)N
μ-LED excitation that was powered with 1.8 μA μm^{-2}
current. We note the particularly low ratio of the back-
ground μ-LED spectral tail to the narrow emission line
intensity. Any uncorrelated photons detected in the
Hanbury-Brown-Twiss experiment would proportionally
reduce the amplitude of coincidence dip as well as the
feasibility of our device as a single-photon source.

The acquired photon coincidence correlation function,
$g_2(\tau)$, is presented in Figure 4b. The photon coin-
cidence correlation function $g_2(\tau)$ denotes the relative
probability density of an event with a time separation
τ. The decrease in the g_2 value around $\tau = 0$ evi-
dences the single-photon component in the emission. The
emission has predominantly single-photon characteristics
when $g_2(0) < 0.5$.

The amplitude of the correlation function at zero de-
lay is significantly low ($g_2(0) = 0.22$), which attests to
the single-photon character of the emission. The pho-
ton coincidence correlation can also be used to deter-
mine the lifetime of the emitter state (Figure 4b). The
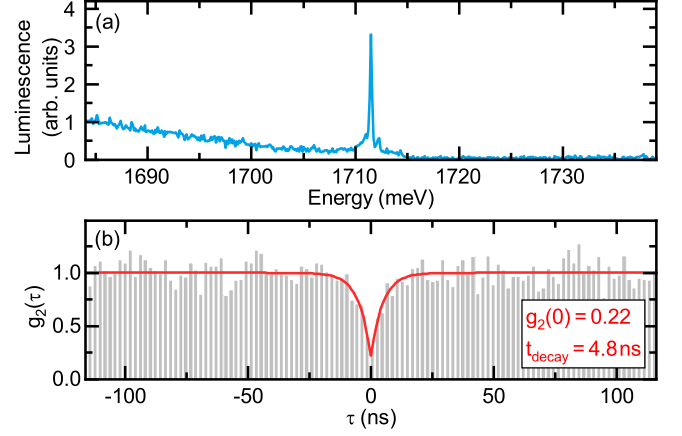lifetime is equal to the characteristic decay time of the

FIG. 4: (a) Luminescence spectrum of the narrow emission
line chosen for the single-photon correlation experiment. (b)
Coincidence correlation counts as a function of the time inter-
val between photons. The photoluminescence is excited with
μ-LED. The broad background luminescence from the μ-LED
was not subtracted in the post-processing.

antibunching feature in the $g_2(\tau)$ profile at the low pho-
ton rate limit. The lifetime obtained in our experiment
($t_{decay} = 4.8$ ns) is in agreement with the results obtained
in other studies[9,13,37–39].

We also used the photon coincidence correlation ex-
periment to verify the temporal stability of the emitter.
Fluctuations of either the emitter intensity or the inten-
sity of its excitation source would result in the effect of
photon bunching. We observe no decrease of g_2 at large
τ, confirming the good stability of the emission center
and the μ-LED. We also observed good long-term stabil-
ity of our device. During several days of measurements,
we have observed no significant variation in the emission
efficiency of the selected center.

IV. CONCLUSION

In conclusion, we have demonstrated that light emis-
sion from TMD monolayers can be efficiently generated
when they are directly deposited on, and excited by the
(In,Ga)N μ-LEDs. Our hybrid devices, 100 μm in size,
can be seen as an optional route towards the effective,
electrically driven generation of light from TMD semi-
conductors. The devices equipped with different MoS$_2$,
WSe$_2$, WS$_2$ and MoSe$_2$ monolayers have been shown to
be operational at low temperatures thanks to the unique
design of our (In,Ga)N micro-LEDs. A proof of con-
cept for a new, electrically driven source of single pho-
tons has been demonstrated with one of our (In,Ga)N
μ-LEDs/WSe$_2$-monolayer devices.

[1] Y. You, X.-X. Zhang, T. C. Berkelbach, M. S. Hybertsen, D. R. Reichman, and T. F. Heinz, Nature Physics **11**, 477 (2015).

[2] K. He, N. Kumar, L. Zhao, Z. Wang, K. F. Mak, H. Zhao, and J. Shan, Physical review letters **113**, 026803 (2014).

[3] J. S. Ross, S. Wu, H. Yu, N. J. Ghimire, A. M. Jones, G. Aivazian, J. Yan, D. G. Mandrus, D. Xiao, W. Yao, et al., Nature communications **4**, 1474 (2013).

[4] E. Lorchat, S. Azzini, T. Chervy, T. Taniguchi, K. Watanabe, T. W. Ebbesen, C. Genet, and S. Berciaud, ACS Photonics **5**, 5047 (2018).

[5] K. F. Mak, C. Lee, J. Hone, J. Shan, and T. F. Heinz, Physical review letters **105**, 136805 (2010).

[6] A. Splendiani, L. Sun, Y. Zhang, T. Li, J. Kim, C.-Y. Chim, G. Galli, and F. Wang, Nano letters **10**, 1271 (2010).

[7] H. Zeng, J. Dai, W. Yao, D. Xiao, and X. Cui, Nature nanotechnology **7**, 490 (2012).

[8] K. F. Mak, K. He, J. Shan, and T. F. Heinz, Nature nanotechnology **7**, 494 (2012).

[9] M. Koperski, K. Nogajewski, A. Arora, V. Cherkez, P. Mallet, J.-Y. Veuillen, J. Marcus, P. Kossacki, and M. Potemski, Nature nanotechnology **10**, 503 (2015).

[10] P. Tonndorf, R. Schmidt, R. Schneider, J. Kern, M. Buscema, G. A. Steele, A. Castellanos-Gomez, H. S. van der Zant, S. M. de Vasconcellos, and R. Bratschitsch, Optica **2**, 347 (2015).

[11] M. Brooks and G. Burkard, Physical Review B **97**, 195454 (2018).

[12] J. Kern, I. Niehues, P. Tonndorf, R. Schmidt, D. Wigger, R. Schneider, T. Stiehm, S. Michaelis de Vasconcellos, D. E. Reiter, T. Kuhn, et al., Advanced Materials **28**, 7101 (2016).

[13] S. Kumar, A. Kaczmarczyk, and B. D. Gerardot, Nano letters **15**, 7567 (2015).

[14] A. Branny, S. Kumar, R. Proux, and B. D. Gerardot, Nature communications **8**, 15053 (2017).

[15] Y. Luo, N. Liu, X. Li, J. C. Hone, and S. Strauf, 2D Materials **6**, 035017 (2019).

[16] M. Blauth, M. Jürgensen, G. Vest, O. Hartwig, M. Prechtl, J. Cerne, J. J. Finley, and M. Kaniber, Nano Letters **18**, 6812 (2018), ISSN 1530-6984.

[17] F. Peyskens, C. Chakraborty, M. Muneeb, D. Van Thourhout, and D. Englund, Nature Communications **10**, 4435 (2019), ISSN 2041-1723.

[18] J. Wang, I. Verzhbitskiy, and G. Eda, Advanced Materials **30**, 1802687 (2018), ISSN 1521-4095.

[19] H. Qiu, T. Xu, Z. Wang, W. Ren, H. Nan, Z. Ni, Q. Chen, S. Yuan, F. Miao, F. Song, et al., Nature Communications **4**, 2642 (2013), ISSN 2041-1723.

[20] S. Wang, W. Zhao, F. Giustiniano, and G. Eda, Physical Chemistry Chemical Physics **18**, 4304 (2016), ISSN 1463-9084.

[21] C. Palacios-Berraquero, M. Barbone, D. M. Kara, X. Chen, I. Goykhman, D. Yoon, A. K. Ott, J. Beitner, K. Watanabe, T. Taniguchi, et al., Nature Communications **7**, 12978 (2016), ISSN 2041-1723.

[22] R. S. Sundaram, M. Engel, A. Lombardo, R. Krupke, A. C. Ferrari, P. Avouris, and M. Steiner, Nano Letters **13**, 1416 (2013), ISSN 1530-6984.

[23] Y. Ye, Z. Ye, M. Gharghi, H. Zhu, M. Zhao, Y. Wang, X. Yin, and X. Zhang, Applied Physics Letters **104**, 193508 (2014), ISSN 0003-6951.

[24] R. Cheng, D. Li, H. Zhou, C. Wang, A. Yin, S. Jiang, Y. Liu, Y. Chen, Y. Huang, and X. Duan, Nano Letters **14**, 5590 (2014), ISSN 1530-6984.

[25] F. Withers, O. Del Pozo-Zamudio, A. Mishchenko, A. P. Rooney, A. Gholinia, K. Watanabe, T. Taniguchi, S. J. Haigh, A. K. Geim, A. I. Tartakovskii, et al., Nature Materials **14**, 301 (2015), ISSN 1476-4660.

[26] S. Wang, J. Wang, W. Zhao, F. Giustiniano, L. Chu, I. Verzhbitskiy, J. Zhou Yong, and G. Eda, Nano Letters **17**, 5156 (2017), ISSN 1530-6984.

[27] D. Li, R. Cheng, H. Zhou, C. Wang, A. Yin, Y. Chen, N. O. Weiss, Y. Huang, and X. Duan, Nature Communications **6**, 7509 (2015), ISSN 2041-1723.

[28] T. Wu, C.-W. Sher, Y. Lin, C.-F. Lee, S. Liang, Y. Lu, S.-W. Huang Chen, W. Guo, H.-C. Kuo, and Z. Chen, Applied Sciences **8**, 1557 (2018).

[29] W. Pacuski, M. Grzeszczyk, K. Nogajewski, A. Bogucki, K. Oreszczuk, J. Kucharek, K. E. Połczyńska, B. Seredyński, A. Rodek, R. Bożek, et al., Nano Letters **20**, 3058 (2020), ISSN 1530-6984.

[30] J. Day, J. Li, D. Y. C. Lie, C. Bradford, J. Y. Lin, and H. X. Jiang, Applied Physics Letters **99**, 031116 (2011), ISSN 0003-6951.

[31] Z. Chen, S. Yan, and C. Danesh, Journal of Physics D: Applied Physics **54**, 123001 (2021), ISSN 0022-3727.

[32] C. Skierbiszewski, H. Turski, M. Zak, K. Nowakowski-Szkudlarek, G. Muziol, M. Siekacz, A. Feduniewicz-Zmuda, and M. Sawicka, in *2018 76th Device Research Conference (DRC)* (2018), pp. 1–2.

[33] S. J. Kowsz, E. C. Young, B. P. Yonkee, C. D. Pynn, R. M. Farrell, J. S. Speck, S. P. DenBaars, and S. Nakamura, Optics Express **25**, 3841 (2017), ISSN 1094-4087.

[34] C. Skierbiszewski, G. Muziol, K. Nowakowski-Szkudlarek, H. Turski, M. Siekacz, A. Feduniewicz-Zmuda, A. Nowakowska-Szkudlarek, M. Sawicka, and P. Perlin, Applied Physics Express **11**, 034103 (2018), ISSN 1882-0786.

[35] M. Chlipala, H. Turski, M. Siekacz, K. Pieniak, K. Nowakowski-Szkudlarek, T. Suski, and C. Skierbiszewski, Optics Express **28**, 30299 (2020), ISSN 1094-4087.

[36] K. Oreszczuk, T. Kazimierczuk, T. Smoleński, K. No-

gajewski, M. Grzeszczyk, A. Łopion, M. Potemski, and P. Kossacki, Physical Review B **102**, 245409 (2020).

[37] A. Srivastava, M. Sidler, A. V. Allain, D. S. Lembke, A. Kis, and A. Imamoğlu, Nature nanotechnology **10**, 491 (2015).

[38] Y.-M. He, G. Clark, J. R. Schaibley, Y. He, M.-C. Chen, Y.-J. Wei, X. Ding, Q. Zhang, W. Yao, X. Xu, et al., Nature nanotechnology **10**, 497 (2015).

[39] C. Chakraborty, L. Kinnischtzke, K. M. Goodfellow, R. Beams, and A. N. Vamivakas, Nature nanotechnology **10**, 507 (2015).